ORIGINAL PAPER

Corrosion inhibition of mild steel in sulfamic acid solution by S-containing amino acids

M. S. Morad

Abstract R_p, potentiodynamic polarization curves and EIS techniques were applied to study the effect of five S-containing amino acids on the corrosion of mild steel in 5% sulfamic acid solution at 40 °C. The compounds are effective inhibitors and the inhibition efficiency follow the order: N-acetylcysteine (ACC) > cysteine (RSH) > S-benzylcysteine (BzC) > cystine (RSSR) $\cong$ methionine (CH$_3$SR). The inhibitors affect the anodic dissolution of steel by blocking the anodic sites of the surface. EIS measurements indicated that charge transfer is the rate determining step in the absence and presence of the inhibitors and the steel/solution interface can be represented by the equivalent circuit $R_s(R_{ct}Q_{dl})$. Adsorption of RSH, CH$_3$SR and RSSR follows the Langmuir model while the Temkin isotherm describes the adsorption of ACC and BzC. From the application of the Flory–Huggins isotherm, the number of water molecules displaced by the adsorbing inhibitor molecules was estimated. The potential of zero charge *pzc* of mild steel without and with the inhibitors is calculated and the mechanism of corrosion inhibition is discussed in the light of the molecular structure.

Keywords Adsorption · Amino acids · Corrosion inhibition · EIS · Mild steel · Potential of zero charge · Sulfamic acid

1 Introduction

Sulfamic acid (H$_2$NSO$_3$H, mono amido sulfuric acid) has long been used as an industrial cleaning agent due to its remarkable property of solubilizing hard scales and deposits. Furthermore, it can be used on mild steel with no problem of pitting or chloride-induced stress corrosion cracking (SCC). Sulfamic acid has the following properties:

- The pure crystals are non-volatile, non-hygroscopic and odorless.
- It is highly stable and can be kept for years without any change in properties.
- It behaves as a strong acid in aqueous solutions but the corrosion rates are significantly lower in comparison to other acids.
- The aqueous solution of sulfamic acid do not emit corrosive fumes, solubilizes hard scales and forms soluble compounds with most industrial deposits.

Because of these properties, acid cleaners based on sulfamic acid are extensively used in a large variety of household and industrial applications e.g., multistage flash evaporators (MSF) seawater desalination plants, heat exchangers and cooling water systems [1, 2].

Our previous investigations showed that amino acids containing sulfur are effective inhibitors for many corrosion systems [3–9]. In this study, five amino acids containing sulfur were tested as inhibitors for mild steel corrosion in 5% sulfamic acid solution at 40 °C. The compounds examined were cysteine (RSH), methionine (CH$_3$SR), cystine (RSSR), N-acetylcysteine (ACC) and S-benzylcysteine (BzC). Linear polarization resistance (R_p), potentiodynamic polarization curves (Tafel plots) and electrochemical impedance spectroscopy (EIS) were employed.

2 Experimental

Electrochemical measurements were conducted in a conventional three-electrode thermostated cell assembly using

M. S. Morad (✉)
Electrochemistry Research Laboratory, Department of Chemistry, Faculty of Science, Assiut University, Assiut 71516, Egypt
e-mail: morad60@aun.edu.eg; mmorad04@yahoo.com

an EG&G potentiostat/galvanostat (model 273) and a lock-in amplifier (model 5210), operated with Corr M352 and EIS M398 software. A platinum sheet with large surface area and standard calomel electrode (SCE) were used as counter and reference electrodes, respectively. To avoid contamination with Cl^- ion, the SCE was coupled to a Luggin capillary filled with the corrosive electrolyte. The tip of the Luggin capillary was located very close to the working electrode (~1 mm distance). Polarization resistance measurements were conducted in the potential range (-15 mV $\leq E_{corr} \leq 15$ mV) with a scan rate of 1 mV s^{-1}. E_{corr} represents the open circuit corrosion potential. Cathodic and anodic polarization curves were traced at a scan rate of 0.25 mV s^{-1} in the potential range -175 to 120 mV versus E_{corr}.

The impedance spectra were collected at the open-circuit corrosion potential (E_{corr}). A single sine wave of 5 mV amplitude was used in the frequency range 0.1 Hz–100 kHz with five points per decade. The results were mathematically modeled using EQUIVCRT by Boukamp [10]. Depending on the concentration of the additives, values of the steady state E_{corr}, were attained in 10–15 min. To ensure the stability of E_{corr}, the working electrode was maintained at its corrosion potential for 5 min in sulfamic acid solution.

Prior to each experiment the working electrode was wet polished with emery paper up to grade 600, rinsed with bi-distilled water, acetone, bi-distilled water and then transferred wet to the cell, already filled with 200 mL of 5% sulfamic acid solution. The latter was deaerated by purified nitrogen for 1 h prior to insertion of the working electrode; purging with nitrogen continued during the course of the experiments. The temperature of the electrolyte was 40 ± 0.2 °C.

The corrosive electrolyte was prepared by dissolving the appropriate amount of pure sulfamic acid (Merck) in bi-distilled water. S-containing amino acids (Merck or Aldrich) were used without further purification in the concentration range 10–1,000 μM by dissolving the amino acid in the sulfamic acid solution. All experiments were conducted in stirred solutions.

The structure of the investigated compounds is shown in Fig. 1:

3 Results and discussion

3.1 Effect of the inhibitor concentration

3.1.1 Open-circuit corrosion potentials (E_{corr})

Figure 2 shows the variation of E_{corr} values (expressed as ΔE_{corr}, $\Delta E_{corr} = E_{corr} - E_{corr}^{inh}$ where E_{corr} and E_{corr}^{inh} are the
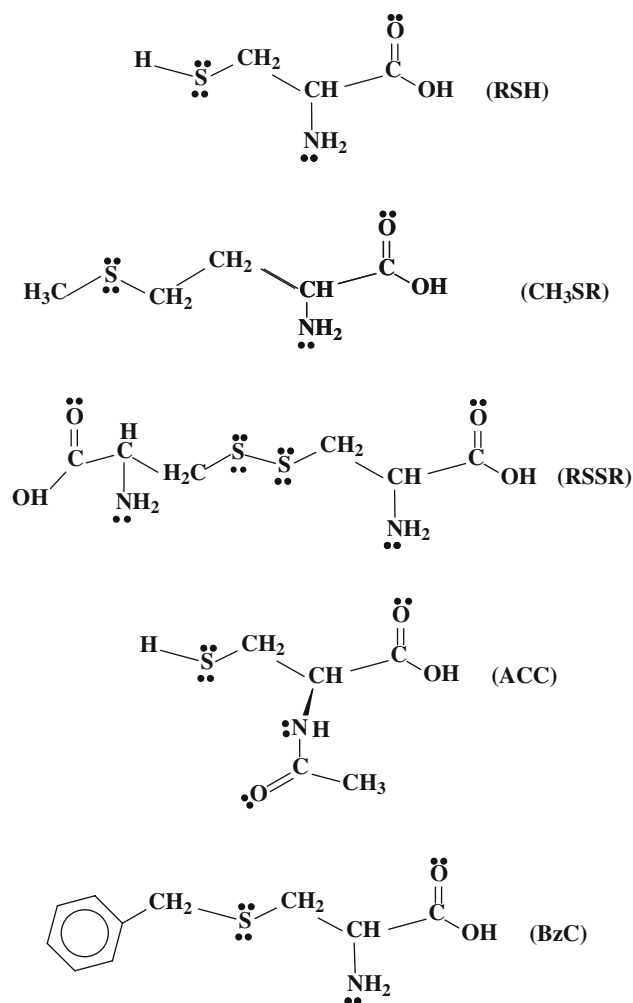

Fig. 1 Structure of the S-containing amino acids
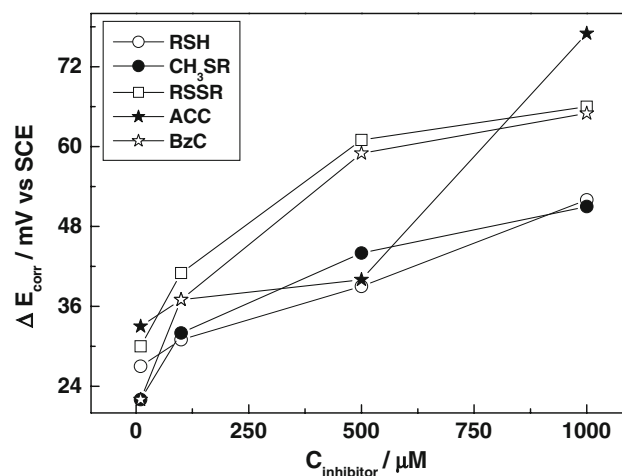

Fig. 2 Variation of ΔE_{corr} of mild steel with the concentration of S-containing amino acids in 5% H_2NSO_3H solution at 40 °C

corrosion potentials in the absence and presence of amino acid) with the concentration of amino acid. All amino acids shift the corrosion potential in the positive direction even at
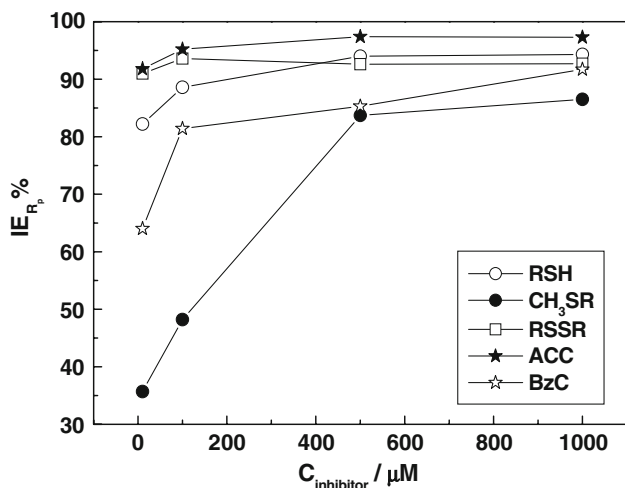
the lowest concentration (10 μM). The positive shift of E_{corr} is increased with increasing amino acid concentration reaching its maximum value at 1,000 μM. At 10 and 1,000 μM concentrations, the maximum displacement of E_{corr} is obtained with ACC. The positive shift of E_{corr} values indicates that amino acids are adsorbed on anodic sites and, consequently, affect mainly the anodic dissolution of iron (see below). The effect of the amino acids on the corrosion potential of mild steel in H_2NSO_3H is similar to their effects in and H_2SO_4 [4] and H_3PO_4 [6] solutions.

3.1.2 R_p measurements

R_p studies showed that addition of 10−1,000 μM RSH, CH_3SR, RSSR, ACC and BzC greatly enhances the value of R_p obtained in the blank solution ($R_p = 15.5$ Ω cm^2) indicating their inhibitive action. In the presence of RSH and ACC, R_p increases with increasing additive concentration up to 500 μM and then slightly decreases. The maximum values of R_p are 257.4 and 606 Ω cm^2 for RSH and ACC, respectively. For CH_3SR and BzC, values of R_p increase with increasing additive concentration reaching a maximum at 1,000 μM. These values amount to 115.2 and 188 Ω cm^2 for CH_3SR and BzC, respectively. In the case of RSSR, the maximum value of R_p is obtained at 100 μM (242.7 Ω cm^2) and increasing concentration results in decreasing polarization resistance. The inhibition efficiency (IE%) was estimated from R_p values according to the equation:

$$IE\% = \left[\left(R_p^1 - R_p^0 \right) / R_p^1 \right] \times 100 \qquad (1)$$

where R_p^0, and R_p^1 are the polarization resistance in the absence and presence of additive, respectively. Figure 3 shows the variation of IE% obtained from R_p with the

concentration of RSH, CH_3SR, RSSR, ACC and BzC. At the highest examined concentration the IE% of amino acids can be ranked as follows:
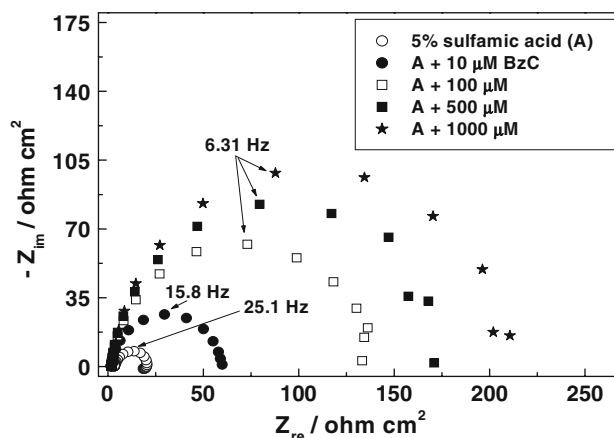
ACC (97.3%) > RSH (94.3%) > RSSR (92.7%) > BzC (91.7%) > CH_3SR (86.5%).

3.1.3 EIS measurements

3.1.3.1 Nyquist plots
Figure 4 shows the impedance diagrams (presented as Nyquist plots) obtained for BzC as a representative example. According to Epelboin et al. [11], the impedance spectra for metal corrosion in acid solutions in the presence of inhibitors can be interpreted in terms of the charge transfer resistance (R_{ct}). On the other hand, electrochemical theory shows that the reciprocal of R_{ct} is directly proportional to the corrosion rate and is analogous to the polarization resistance (R_p) in the Stern–Geary equation.

For the uninhibited solution in Fig. 4, the Nyquist plot is composed of a capacitive loop covering most of the frequency range, followed by a small inductive loop below 1 Hz. The inductive loop is commonly associated with the relaxation process of adsorbed species at the metal/solution interface. The capacitive loop can be ascribed to charge transfer. In the presence of 10–1,000 μM BzC, only one semicircle is observed. The diameters of the semicircles increase (and hence the value of R_{ct}) with increasing concentration of BzC indicating its inhibition effect. RSH, CH_3SR, RSSR, ACC show the same behavior with the difference that:

1. In the presence of RSH and ACC, the diameter of the capacitive loop increases with increasing additive concentration up to 500 μM and then decreases.

Fig. 3 Variation of the inhibition efficiency calculated from R_p values with the concentration of S-containing amino acids

Fig. 4 Complex plane impedance of mild steel recorded in 5% H_2NSO_3H solution without and with different concentrations of BzC. Spectra recorded at E_{corr} (40 °C)

2. For CH_3SR and BzC, the diameter of the capacitive loop increases with increasing additive concentration reaching a maximum at 1,000 μM.
3. For RSSR, the maximum increase of the capacitive loop is obtained at 100 μM and increasing the concentration results in decreasing diameter.

In the presence of amino acids, depressed semicircles are noticed while the inductive loop shown in the spectrum recorded in the blank solution disappears. The depressed capacitive loops decrease with increasing inhibitor concentration. This type of diagram is usually interpreted as indicating a mechanism of charge transfer on a non-homogeneous surface [12].

3.1.3.2 Quantitative analysis of the impedance spectra For the purpose of impedance spectra analysis, the experimental data were fitted using the Boukamp equivalent circuit program [10]. Regardless of the inductive loop that appeared in the pure solution, the experimental data were found to fit well the equivalent circuit $R_s(R_{ct}Q_{dl})$ proposed in previous studies on steel corrosion in acid media [7, 8, 13–15]. This consists of a solution resistance R_s, a charge transfer resistance R_{ct} and a constant phase element *cpe*, which is related to the capacity of the double layer C_{dl}. The *cpe* is composed of a component Q_{dl} and a coefficient *n*. The coefficient *n* can characterize different surface phenomena such as surface heterogeneity resulting from surface roughness, impurities, inhibitor adsorption or porous layer formation [16, 17]. Values of the impedance parameters R_s, R_{ct}, Q_{dl} and *n* were calculated and are given in Table 1. The reliability of the proposed equivalent circuit is determined by the relative errors of the fitted parameters. Values of the relative error in the absence and presence of amino acids range from 0.5 to 8%, which indicate good correlation between experimental and fitted data.

From Table 1, it is clear that addition of BzC causes a significant increase in R_{ct} in the additive-free solution and diminishes the value of Q_{dl}. These findings indicate that

BzC inhibits mild steel corrosion by adsorption. As the impedance spectra show one capacitive loop, adsorption of BzC occurs by simple surface coverage and BzC acts as a primary interface inhibitor [18]. Increasing the coefficient *n* with increase in BzC concentration reflects decreased heterogeneity of the mild steel surface as a result of adsorption of BzC. Similar impedance spectra were obtained in the presence of RSH, CH_3SR, RSSR and ACC but differ in the following:

1. Values of R_{ct} obtained in the presence of RSH and ACC increase with increasing additive concentration up to 500 μM and then decrease.
2. For CH_3SR and BzC, values of R_{ct} increase with increasing additive concentration reaching a maximum at 1,000 μM.
3. For RSSR the maximum increase in R_{ct} is obtained at 100 μM after which it decreases.
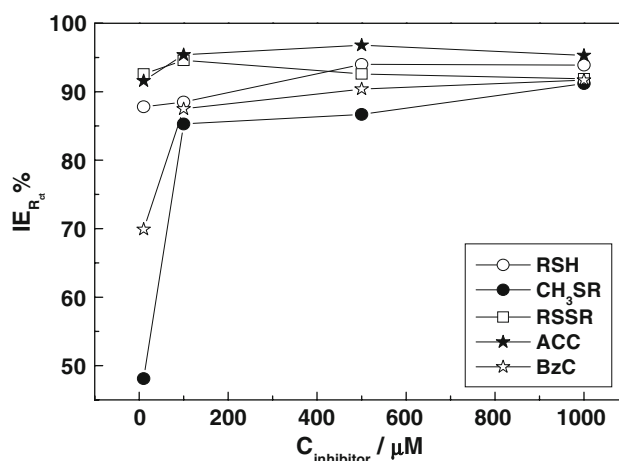
3.1.3.3 Inhibition efficiency (IE%) Values of R_{ct} estimated from the above-mentioned equivalent circuit were used to calculate IE% according to the following equation:

$$IE\% = \left[\left(R_{ct}^1 - R_{ct}^0 \right) / R_{ct}^1 \right] \times 100 \quad (2)$$

where R_{ct}^0, and R_{ct}^1 are the charge transfer resistances in the absence and presence of additive respectively. Figure 5 shows the variation of IE% obtained from R_{ct} with the concentration of RSH, CH_3SR, RSSR, ACC and BzC. At the highest examined concentration, the IE% of amino acids can be ranked as follows:

ACC (95.3%) > RSH (93.9%) > RSSR (91.9%) $\cong$ BzC (91.7%) $\cong$ CH_3SR (91.2%).

These results agree reasonably with those of R_p measurement and both techniques show that ACC is the best inhibitor among the amino acids studied.

Table 1 R_p and EIS parameters of mild steel in 5% sulfamic acid without and with BzC

[BzC] (μM)	R_p		EIS				
	R_p^a	IE%	R_s^a	R_{ct}^a	Q_{dl} ($\times 10^{-4}$)[b]	*n*	IE%
0	13.8	–	3.43	17.4	4.0	0.94	–
10	43.1	68	1.75	57.8	2.32	0.94	69.9
100	92	85	1.71	139	2.30	0.93	87.5
500	105.4	86.9	1.81	181	1.97	0.95	90.4
1000	188	92.6	2.32	210.3	1.63	0.97	91.7

[a] Ω cm^2, [b] Ω^{-1} cm^{-2} s^n

Fig. 5 Variation of the inhibition efficiency calculated from R_{ct} values with the concentration of S-containing amino acids

3.1.4 Potentiodynamic polarization curves

Figure 6 shows the anodic and cathodic polarization curves obtained in the absence and presence of 10–1,000 μM RSH (representative curves). Addition of 10 μM RSH slightly shifts the cathodic curve of the blank to lower current densities indicating inhibition of the hydrogen evolution reaction. Further additions do not disturb the cathodic reaction. In the anodic domain, it is evident that the curve recorded in the pure medium is markedly shifted towards lower current densities indicating a strong inhibition effect of the anodic reaction (iron dissolution). The same behavior was observed in the presence of the remaining compounds, except CH_3SR, where the shift of the anodic curves towards lower current densities is much less in comparison to the remaining amino acids.

Kinetic corrosion parameters such as anodic (b_a) and cathodic ($-b_c$) Tafel slopes, as well as the corrosion current density (i_{corr}) were estimated separately. Careful analysis of the corrosion parameters showed that values i_{corr} could not be calculated from the intersection of the Tafel regions of the polarization curves (except in the case of the pure medium) at the corrosion potentials. Unusually they intersect at values more positive than those of E_{corr} by ~ 15 mV and thus erroneous values of i_{corr} are obtained. Consequently, values of b_a and $-b_c$ were calculated by linear fitting of the Tafel regions of the anodic and cathodic branches of each polarization curve and were used to calculate values of i_{corr} according to the Stern–Geary equation [19]:

$$i_{corr} = \left\{ (|b_a \times b_c|) / [2.303\, R_p(|b_a + b_c|)] \right\} \quad (3)$$

Values of R_p are those obtained from linear polarization measurements.

Corrosion parameters obtained in the absence and presence of 10 and 1,000 μM RSH, CH_3SR, RSSR, ACC and BzC are given in Table 2. In the pure solution, values of b_a and b_c amount to 56 and -166 mV decade^{-1}, respectively. These values are close to those obtained for mild steel corrosion in mineral acids [7, 20–22]. In the presence of 10 μM RSH, RSSR, ACC and BzC, values of b_a and b_c obtained in blank solution are significantly decreased and by increasing the inhibitor concentration, they again increase. For CH_3SR, although an initial decrease in b_a and b_c is observed at 10 μM, further increase in additive concentration does not lead to any remarkable change. The marked decrease in values of anodic and cathodic Tafel slopes may be attributed to two effects:

(i) An energy effect: Addition of inhibitor lowers the overpotential of both anodic and cathodic reactions due to inhibitor adsorption [23].

(ii) Desorption effect: For the anodic reaction, in addition to the energy effect, the pronounced decrease in b_a may be partly due to electrochemical desorption of the inhibitor from the steel surface during dissolution [24].

Table 2 reveals that all amino acids markedly decreased the value of i_{corr} obtained in the inhibitor-free solution indicating their powerful inhibitive effect.

Values of i_{corr} were used to calculate the inhibition efficiency using the following equation:

$$IE\% = \left[(i_{corr}^0 - i_{corr}^1) / i_{corr}^0 \right] \times 100 \quad (4)$$

where i_{corr}^0 and i_{corr}^1 are the corrosion current density in the absence and presence of the additive respectively. Figures 7, 8 show the variation of IE% with the concentration of RSH, CH_3SR, RSSR, ACC and BzC. At the highest examined concentration, the IE% of amino acids can be arranged as follow:
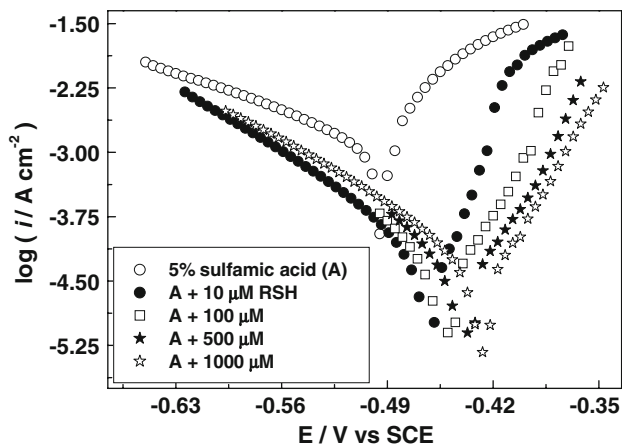

Fig. 6 Potentiodynamic polarization curves of mild steel recorded in 5% H_2NSO_3H solution without and with different concentrations of RSH at 40 °C

Table 2 Corrosion kinetic parameters of mild steel in 5% sulfamic acid in absence and presence of 10 and 1,000 μM amino acid concentrations

Amino acid	b_a*	$-b_c^a$	i_{corr} (μA cm^{-2})	IE%
Blank	56	166	1,173	–
10 μM RSH	18	89	73	93.8
1,000 μM	32	97	39	96.7
10 μM CH_3SR	16	91	245	79.1
1,000 μM	15	88	48.3	95.9
10 μM RSSR	18	93	38	96.8
1,000 μM	45	188	74	93.7
10 μM ACC	33	109	57.8	95.1
1,000 μM	65	113	30.8	97.4
10 μM BzC	38	91	270	77
1,000 μM	67	159	108.9	90.7

^{a} mV decade^{-1}
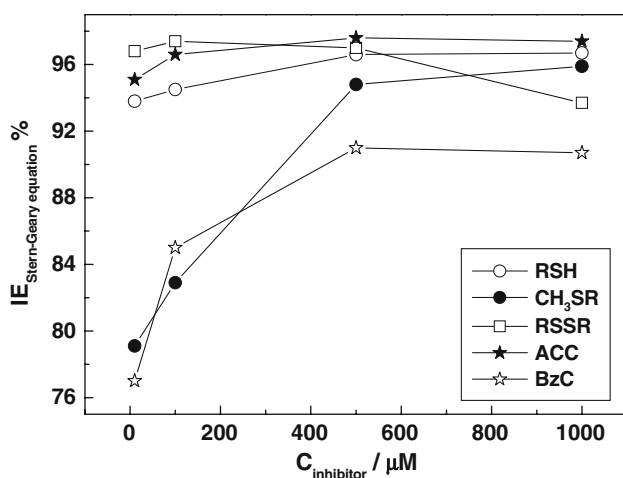
Fig. 7 Variation of the inhibition efficiency (calculated from Stern–Geary equation) with the concentration of S-containing amino acids
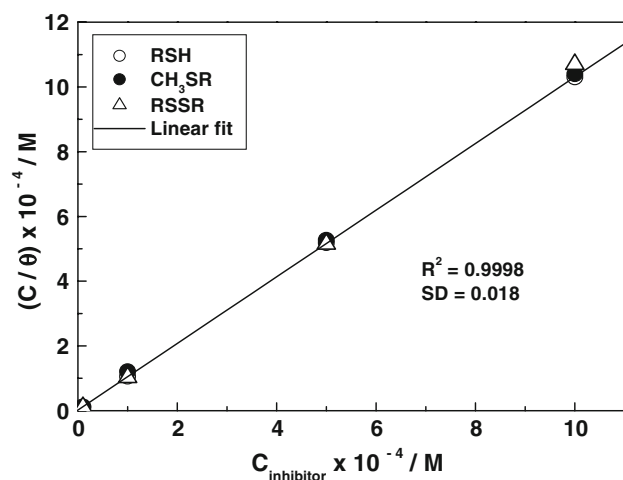

Fig. 8 Langmuir adsorption isotherms of RSH, CH$_3$SR and RSSR on mild steel surface in 5% H$_2$NSO$_3$H solution at 40 °C

ACC (97.4%) > RSH (96.7%) > CH$_3$SR (95.9%) > BzC (93.7%) > RSSR (90.7%).

The above order differs partly from those obtained from R$_p$ and EIS. The difference may be attributed to the change in surface state during polarization, which plays an important role in the adsorption process.

3.2 Adsorption isotherms

In aqueous solution, the adsorption of an organic inhibitor at an electrode/electrolyte interface may be considered in terms of the displacement of adsorbed water molecules at the inner Helmholtz plane of the electrode, viz.

$$Org_{(aq)} + x\,H_2O_{(ads)} \rightleftharpoons Org_{(aq)} + x\,H_2O_{(ads)} \tag{5}$$
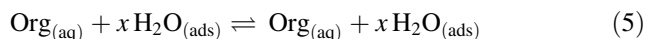
Assuming that the steel electrode corrodes uniformly, the corrosion current density in the blank solution is representative of the total number of corroding sites. Also, the corrosion current density in the presence of the inhibitor is representative of the number of available corroding sites remaining after blockage of some sites due to inhibitor adsorption. The modeling of these assumptions enable a derivation for the fractional surface coverage (θ), viz.

$$\theta = \left(i_{corr}^0 - i_{corr}^1\right)/i_{corr}^0 \tag{6}$$

Values of θ obtained by equation were subjected to several adsorption isotherms and it was found that RSH, CH$_3$SR and RSSR fit the Langmuir adsorption isotherm, where θ and the inhibitor concentration C are related via the equation:

$$\theta = KC/(1 + KC) \tag{7}$$

Rearrangement gives

$$C/\theta = (1/K) + C \tag{8}$$

where K is the adsorption constant.

Figure 8 shows the plot of C/θ against C for the three compounds. The linear fit of the data is also included. The strong correlation coefficient ($R^2 = 0.9998$) confirms the validity of the isotherm. The slope of the fitted line is 1.04 which is in accord with the assumption in the derivation of the Langmuir isotherm that the active substrate sites accommodate only one molecule. The adsorption constant K is related to the standard free energy change of adsorption (ΔG_{ads}°) by the equation [5]:

$$K = (1/55.5) \exp\left(-\Delta G_{ads}^\circ/RT\right) \tag{9}$$

On the other hand, values of θ calculated for ACC and BzC were found to fit the Temkin adsorption isotherm (Fig. 9) where θ varies linearly with log C (C is the molar concentration of the inhibitor in the bulk of solution) indicating monolayer adsorption. Figure 9 shows that adsorption of both ACC and BzC follows the Temkin
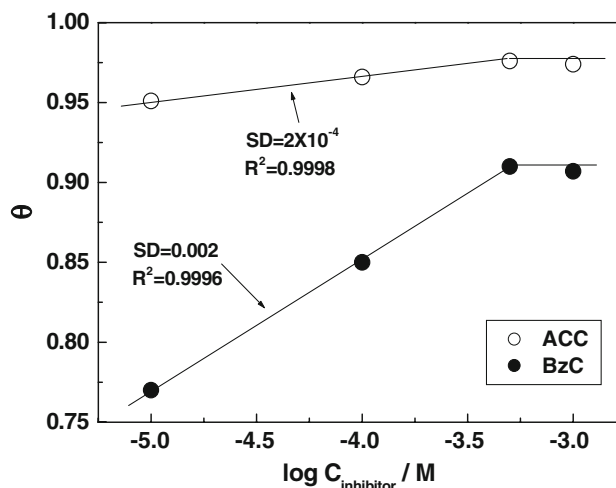
Fig. 9 Temkin adsorption isotherms of ACC and BzC on mild steel surface in 5% H$_2$NSO$_3$H solution at 40 °C

Table 3 Adsorption parameters of S-containing amino acids on mild steel surface in 5% sulfamic acid solution at 40 °C (as calculated from Stearn–Geary equation)

Amino acid	K (M^{-1})	ΔG°_{ads} (kJ mol^{-1})	Parameters derived from Flory–Huggins isotherm		
			x	K (M^{-1})	ΔG°_{ads} (kJ mol^{-1})
RSH	7×10^5	−45.45	4.1	3.63×10^8	−61.7
CH$_3$SR	9.95×10^4	−40.38	2.7	2.04×10^6	−48.24
RSSR	1.85×10^5	−42	–	–	–
ACC	5.1×10^{30}	−194.3	7.35	4.36×10^{13}	−92.13
BzC	2.03×10^{14}	−96.1	4.4	9.17×10^6	−52.14

isotherm up to 500 μM after which a saturation limit is observed. The different adsorption behavior exerted by the amino acids may be ascribed to the difference in their molecular structures.

The adsorption parameters K and ΔG°_{ads} were calculated and are given in Table 3. These values follow the order: ACC ≫ BzC ≫ RSH > RSSR > CH$_3$SR. The high values of K indicate electrical interaction between the double layer at the phase boundary and the adsorbing inhibitor molecules. The large negative values of ΔG°_{ads} indicate that the adsorption reaction proceeds spontaneously and is accompanied by highly efficient adsorption.

Values of f were found to be 156 and 28 for ACC and BzC. It was reported [25] that the interaction factor may have two values: a positive value (f > 0) indicates lateral attractive interaction between adsorbed molecules and a negative value (f < 0) reflects the presence of lateral repulsive interaction between the adsorbed molecules. Thus there is a strong attractive lateral interaction between the adsorbed ACC or BzC molecules on the steel surface. The lateral attractive interaction between ACC molecules is stronger than that between BzC molecules.

The highest values of K, $-\Delta G^{\circ}_{ads}$ and f obtained for ACC suggests that ACC is the most efficient inhibitor among the investigated amino acids.

Equation 5 signifies that the adsorption of an inhibitor on the electrode surface is a substitutional process in which the adsorbing inhibitor molecule replaces a number, x, of water molecules from the surface. Thus, trials were carried out to estimate x by fitting values of θ to isotherms that take x into consideration. These isotherms include the Bockris–Swinkel (BS) [26], Flory–Huggins (FH) [27] and multisites Langmuir (MSL) [28] isotherms. The parameter n in the MSL model is equal to the parameter x in the FH model. It was found that the FH isotherm satisfactorily fits the experimental data obtained for RSH, CH$_3$SR, ACC and BzC.

The Flory–Huggins adsorption isotherm is given by the equation

$$\theta / [x(1-\theta)^x] = KC \tag{10}$$

Rearrangement gives

$$\log(\theta/C) = \log m + x\log(1-\theta) \tag{11}$$
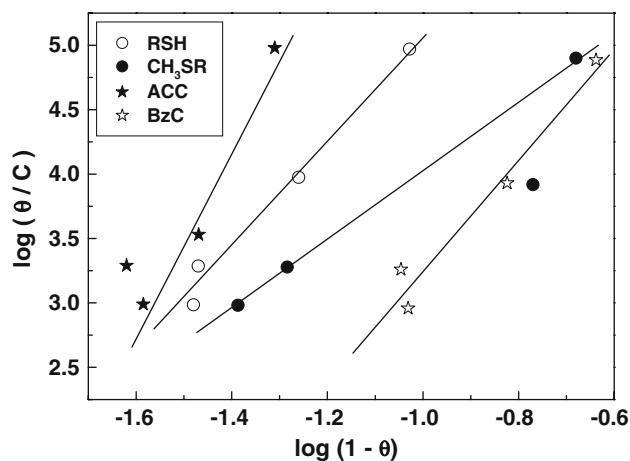
Fig. 10 Flory–Huggins isotherms of S-containing amino acids on mild steel surface in 5% H$_2$NSO$_3$H solution at 40 °C

where log m = log K + log x. The plot of log (θ/C) versus log (1 − θ) should give a straight line from which values of both x and K may be estimated. Figure 10 shows the FH isotherms obtained for RSH, CH$_3$SR, ACC and BzC while the associated adsorption parameters are listed in Table 3. None of the above-mentioned isotherms is applicable to the data of RSSR since no straight line was obtained. Data interpretation according to the FH model suggests that one ACC molecule replaces 7 water molecules from the steel surface while a molecule of CH$_3$SR replaces only three water molecules. Again the highest values of K and ΔG°_{ads} are obtained in the presence of ACC and provide further evidence that ACC is the best inhibitor among the studied S-containing amino acids.

3.3 Potential of zero charge (*pzc*) of mild steel in sulfamic acid solution

It is well established that the inhibition efficiency of chemically stable surface-active compounds is related primarily to their ability to adsorb on the metal-solution interface. For a given solution the adsorbability of inhibitors will depend first of all on the charge of the metal or, more precisely, on the potential of the metal on the

correlative scale (φ_c-scale). The value of φ_c is given by the equation [29]:

$$\varphi_c = E_{corr} - E_{q=0} \qquad (12)$$

$E_{q=0}$ is known as the potential of zero charge (*pzc*)

The value of *pzc* of mild steel in sulfamic acid was determined using EIS. Impedance spectra at different polarization potentials were recorded in the absence and presence of 10 μM RSSR. Nyquist plots have the same shape as those presented in Fig. 4. The capacitive loop in the high frequency region usually originates from the relaxation of the double-layer capacitance under the following conditions:

(i)   There are no rapid pseudo-capacitive processes, which can be coupled with the double layer relaxation [30].
(ii) There is no specific adsorption of anions.

The two conditions can be met in sulfamic acid solution. Thus, EIS offers a good method to determine the *pzc* of mild steel in H_2NSO_3H solution. We have measured a series of impedance spectra in a relatively wide potential range between −675 and −350 mV versus SCE. These were analyzed using the EQUIVCRT program [10] and the plots of C_{dl}/E are shown in Fig. 11 (representative curves). The minima of these curves in the absence and presence of 10 μM RSSR is considered as the *pzc*. As can be seen from the values of *pzc* marked in Fig. 11, these values lie at potentials more negative than the corresponding values of E_{corr}. So, values of φ_c of mild steel in the absence and presence of RSSR are positive and hence the steel surface is positively charged. Accordingly, the protonated amino acids could not be adsorbed on steel at the free-corrosion potential.
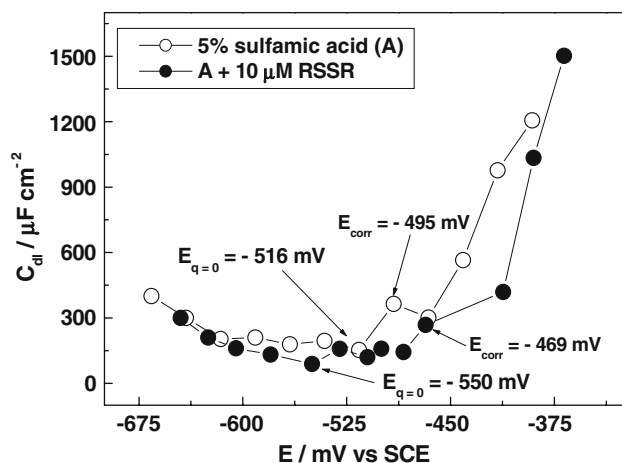
Fig. 11 Relation between double layer capacitance C_{dl} with the applied potential on mild steel electrode immersed in 5% H_2NSO_3H solution without and with 10 μM RSSR

4 Mechanism of corrosion inhibition by S-containing amino acids

As previously mentioned the adsorption of S-containing amino acids on the positively charged steel surface cannot take place through the positively charged nitrogen atom (amino acids undergo protonation through the −NH_2 group in acid solution). Therefore, it is assumed that, at least in the first few minutes of contact between the substrate and the solution, they exist as cationic species at the interface [7]. At E_{corr} it is suggested that sulfamate ions ($H_2NSO_3^-$) are preferentially adsorbed and then coulombic interaction between sulfamate ion and protonated amino acid takes place (physical adsorption). Such adsorption will be increased owing to the presence of several adsorption centers (at least three centers, namely N, S and O atoms in each amino acid). In this case, beside the physical adsorption, chemisorption via N, S and O atoms occurs on the anodic sites. This may explain the high inhibition efficiency of amino acids as impedance spectra show (Fig. 4).

Under cathodic polarization conditions adsorption of the cationic species on the negatively charged surface occurs via electrostatic attraction. The resulting physical adsorption is not so strong as to impart high inhibition efficiency. This may explain the slight shift of the cathodic branches of the polarization curves towards low values of current density (Fig. 6).

Under anodic polarization conditions, the high inhibition efficiency of these compounds may be ascribed to their adsorption on the anodic sites of the surface via the sulfur atom. According to Trabanelli [31], the sulfur atom is less polarizable and has better donation for the lone pair of electrons than the nitrogen atom. So, the most probable adsorption center is the S atom. Donation of a pair of unshared electrons to an unoccupied d-orbital of the Fe atom results in the formation of a chemisorbed bond. Since the investigated compounds are electron donors and the Fe atoms on the surface are electron acceptors, they are equivalent to Lewis bases and acids, respectively, and the inhibition effects of the compounds are expected to be related to the hard and soft acids and bases (HSAB) principle [32]. Adsorption of the S-containing amino acids on the surface anodic sites is supported by the large positive shift of E_{corr} and the marked displacement of the anodic polarization curves towards low current densities.

S-containing amino acids are adsorbed perpendicularly through the S atom and this leaves the rest of the molecule to be interacted by Van der Wall forces, forming a hood covering the adsorption center. This mode of adsorption hinders diffusion of hydrogen ions from the bulk solution to the metal surface and hence inhibits steel dissolution.

At 1,000 μM concentration, the average of the inhibition efficiency as calculated from the three techniques leads to the following order:

ACC (96.7%) > RSH (95.0%) > BzC (92.4%) > RSSR (91.8%) $\cong$ CH$_3$SR (91.2%).

The highest inhibition efficiency obtained in the presence of ACC suggests that the chemisorbed ACC molecules probably form a chelate compound with the surface iron atoms by coordinate bond formation with both the –SH group and the oxygen atom of the acetyl group. Although the –CH$_3$ group has two electronic effects [33]: an inductive effect (+I) by which the electron density of the carbonyl group is increased, and a steric effect (a sheer physical blockage); it seems that the former effect is more effective than the latter. Therefore, complexation of ACC with the surface is much higher than that obtained by the parent compound RSH.

For BzC, the replacement of the –SH group by the benzyl group is expected to increase the efficiency of BzC by sharing the π-electrons of the phenyl group in the adsorption process. The lower inhibition efficiency of BzC compared to RSH may be ascribed to the rigidity of the benzyl group and the increased molecular size. Therefore, repulsion between the adsorbed BzC molecules within the adsorbed layer takes place and leads to a decrease in the inhibition efficiency.

The presence of two adsorption centers (two sulfur atoms) in RSSR is expected to impart higher inhibition efficiency than RSH. The lower IE% of RSSR than RSH and the decrease in inhibition efficiency at high concentration may be ascribed to increased coulombic repulsion experienced by the inhibitor molecules during adsorption. For large inhibitor molecules, molecular crowding or steric effects have a negative effect on inhibition efficiency.

Although CH$_3$SR has an electron-donor group (–CH$_3$) attached to the adsorption center (S atom), the steric hindrance exerted by this group affects the stability and the performance of the adsorbed layer at the metal/solution interface and consequently, CH$_3$SR provides the lowest inhibition.

The mutual adsorption of amino acid and sulfamate ion on the steel surface may explain the better performance of S-containing amino acids in H$_2$NSO$_3$H than in H$_2$SO$_4$ [4, 8] and H$_3$PO$_4$ [6, 7].

5 Conclusions

(1) Inhibition of mild steel corrosion in sulfamic acid at 40 °C by S-containing amino acids was established from R$_p$, polarization curves and EIS measurements. The three techniques revealed that ACC is the most effective compound while CH$_3$SR gives the lowest inhibition.

(2) EIS showed that charge transfer is the rate-determining step of the corrosion of mild steel in the absence and presence of inhibitors. Impedance spectra can be satisfactorily simulated by a simple interface model having only one time constant, that is, R$_s$(R$_{ct}$Q$_{dl}$).

(3) Polarization curves indicate that S-containing amino acids act essentially as anodic inhibitors in sulfamic acid, retarding the anodic dissolution of steel by blockage of active sites.

(4) Adsorption of RSH, CH$_3$SR and RSSR on steel obeys the Langmuir isotherm while the Temkin isotherm describes the adsorption of ACC and BzC. From application of the Flory–Huggins isotherm, a molecule of ACC replaces 7 water molecules (the highest number) while water molecules (the lowest number) are replaced by one molecule of CH$_3$SR. Negative values of the standard free energy change for the adsorption process indicate chemisorption of the S-containing amino acids via the S-atom. The values of ΔG_{ads}° ranged between -194.3 kJ mol^{-1} (for ACC) and -40.38 kJ mol^{-1} (for CH$_3$SR).

(5) The pzc values in the absence and presence of inhibitors and their comparison with the corresponding values of E$_{corr}$ reveal that the steel surface is positively charged under open circuit conditions.

References

1. Yakovleva LA, Vakulenko LA, Vdovenko ID, Lisogor AI, Kalinyuk NN, Novitskaya GN (1987) Ukr Khim Zhurn [Soviet Progress in Chemistry] 53: 709 and references therein
2. http://www.dmcc.com/sulphamicacid1.html
3. Morad MS (1995) Inhibition and acceleration of mild steel corrosion in pickling acids. PhD thesis, Assiut University
4. Abdel Aal MS, Morad MS, Ahmed ZA (1995) Proc 8th Symp Corros Inhib (8 SEIC). Ann Univ Ferrara, NS Sez V, Suppl 10, p 343
5. Morad MS, Hermas AA (2001) J Chem Technol Biotechnol 76:401
6. Morad MS, Hermas AA, Abdel Aal MS (2002) J Chem Technol Biotechnol 77:486
7. Morad MS (2005) J Appl Electrochem 35:889
8. Morad MS (2007) J Appl Electrochem 37:661
9. Morad MS (2007) J Appl Electrochem 37:1191
10. Boukamp BA (1989) Equivalent circuit (EQUIVCRT, PAS), User's manual second version revised edition. University of Twente
11. Epelboin I, Keddam M, Takenouti H (1972) J Appl Electrochem 2:71
12. Jüttner K (1990) Electrochim Acta 35:1501
13. Lebrini M, Lagrenée M, Vezin H, Traisnel M, Bentiss F (2007) Corros Sci 49:2254
14. Popova A, Christov M, Vasilev A (2007) Corros Sci 49:3290
15. Hassan HH, Abdelghani E, Amin MA (2007) Electrochim Acta 52:6359
16. Veleda S, Popova A, Raicheva S (1990) Proc 7th Europ Symp Corros Inhib (7 ESCI). Ann Univ Ferrara, Ferrara, NS Sez V, Suppl 9, p 363
17. Lorenz WJ (1986), Dechema monographs. Weinheim Verlag Chemie 101:185

18. Fischer H (1972) Werkst Korros 23:445
19. Stern M, Geary AL (1957) J Electrochem Soc 104:56
20. Gowrani T, Yamuna J, Parameswari K, Chitra S (2004) Anti Corros Meth Mater 51:414
21. Sathiyanarayanan S, Jeyaprabha C, Muralidharan S, Venkatachari G (2006) Appl Surf Sci 252:8107
22. Popova A, Christov M, Zwetanova A (2007) Corros Sci 49:2031
23. Martinez S, Metikos-Hukovic M (2003) J Appl Electrochem 33:1137
24. Drazic VJ, Drazic DM (1990) Proc 7th Europ Symp Corros Inhib (7 ESCI). Ann Univ Ferrara, Ferrara, NS Sez V, Suppl 9, p 99
25. Cano E, Polo JL, La Iglesia A, Bastidas JM (2004) Adsorption 10:219
26. Bockris JO'M, Swinkel DA (1964) J Electrochem Soc 111:737
27. Dahr HP, Conway BE, Joshi KM (1973) Electrochim Acta 18:789
28. Kern P, Landolt D (2001) J Electrochem Soc 148:B228 and references therein
29. Antropov LI (1967) Corros Sci 7: 607
30. Barcia OE, Mattos OR (1990) Electrochim Acta 35:1601
31. Trabanelli G (1987) In: Mansfeld F (ed) Corrosion inhibitors in corrosion mechanisms. Marcel Dekker, Inc., New York, Basel, p 127
32. Aramaki K (1983) Boshoku Gijutsu 32:144
33. Popova A, Christov M, Raicheva S, Sokolova E (2004) Corros Sci 46:1333 and references therein